

CRAB WAIST COLLISIONS IN DAΦNE AND SUPER-B DESIGN

P. Raimondi, INFN Laboratori Nazionali Frascati, Frascati, Italy

Abstract

The new idea of increasing the luminosity of a collider with crab waist collisions and first experimental results from the DAΦNE Φ-Factory at LNF, Frascati, using this concept are presented. Consequences for the design of future factories will be discussed. An outlook to the performance reach with crab waist collisions is given, with emphasis on future B Factories.

INTRODUCTION

A novel collision scheme, the “large Piwinski angle and crab waist” [1,2] has been studied, which will allow to reach unprecedented luminosity with low beam currents and reduced background at affordable operating costs. The principle of operation of this scheme is under test at the DAΦNE Frascati Φ-Factory [3].

The scheme finds its natural application to the SuperB project [4] aims at the construction of a very high luminosity ($10^{36} \text{ cm}^{-2} \text{ s}^{-1}$) asymmetric (4 on 7 GeV) e^+e^- Flavour Factory with possible location at the campus of the University of Rome Tor Vergata near the INFN Frascati National Laboratory. A Super-B Conceptual Design Report (CDR) [5] was issued in May 2007.

LARGE PIWINSKI ANGLE AND CRAB WAIST CONCEPT

The Crab Waist scheme of beam-beam collisions can substantially increase collider luminosity since it combines several potentially advantageous ideas.

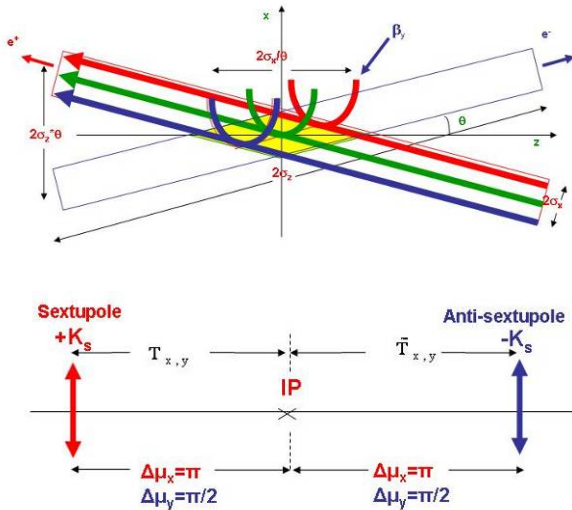


Figure 1: Collision scheme with large Piwinski angle and crabbing sextupoles.

The first one is large Piwinski angle. For collisions under a crossing angle θ the luminosity L and the

horizontal ξ_x and vertical ξ_y tune shifts scale as (see, for example, [6]):

$$L \propto \frac{N\xi_y}{\beta_y} \propto \frac{1}{\sqrt{\beta_y}}; \quad \xi_y \propto \frac{N\sqrt{\beta_y}}{\sigma_z\theta}; \quad \xi_x \propto \frac{N}{(\sigma_z\theta)^2}$$

Here the Piwinski angle is defined as:

$$\phi = \frac{\sigma_z}{\sigma_x} \text{tg}\left(\frac{\theta}{2}\right) \approx \frac{\sigma_z}{\sigma_x} \frac{\theta}{2}$$

with N being the number of particles per bunch. Here we consider the case of flat beams, small horizontal crossing angle $\theta \ll 1$ and large Piwinski angle $\phi \gg 1$.

In the CW scheme described here, the Piwinski angle is increased by decreasing the horizontal beam size and increasing the crossing angle. In such a case, if it were possible to increase N proportionally to $\sigma_z\theta$, the vertical tune shift ξ_y would remain constant, while the luminosity would grow proportionally to $\sigma_z\theta$. Moreover, the horizontal tune shift ξ_x drops like $1/\sigma_z\theta$. However, the most important effect is that the overlap area of the colliding bunches is reduced, as it is proportional to σ_x/θ (see Fig. 1). Then, the vertical beta function β_y can be made comparable to the overlap area size (i.e. much smaller than the bunch length):

$$\beta_y \approx \frac{\sigma_x}{\theta} \ll \sigma_z$$

We get several advantages in this case:

- Small spot size at the IP, i.e. higher luminosity L .
- Reduction of the vertical tune shift ξ_y .
- Suppression of synchrotron resonances [7].

Besides, there are additional advantages in such a collision scheme: there is no need to decrease the bunch length to increase the luminosity as proposed in standard upgrade plans for B- and Φ-factories [8, 9, and 10]. This will certainly help solving the problems of HOM heating, coherent synchrotron radiation of short bunches, excessive power consumption etc. Moreover, parasitic collisions (PC) become negligible since with higher crossing angle and smaller horizontal beam size the beam separation at the PC is large in terms of σ_x .

However, large Piwinski angle itself introduces new beam-beam resonances which may strongly limit the maximum achievable tune shifts (see [11], for example). At this point the crab waist transformation enters the game boosting the luminosity. This takes place mainly due to suppression of betatron (and synchrotron) resonances arising (in collisions without CW) through the vertical motion modulation by the horizontal oscillations [12]. The CW vertical beta function rotation is provided by sextupole magnets placed on both sides of the IP in phase with the IP in the horizontal plane and at $\pi/2$ in the

vertical one (see Fig. 1). A numerical example of the resonance suppression is shown in Fig. 2.

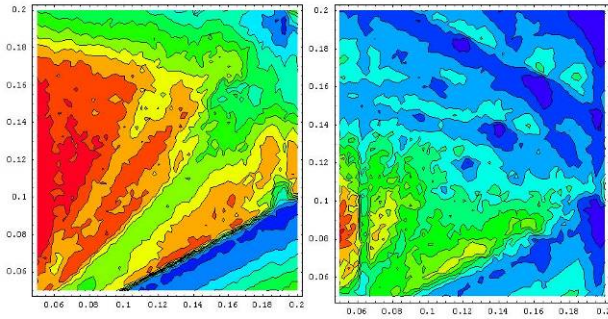


Figure 2: Luminosity tune scan (v_x and v_y from 0.05 to 0.20). CW sextupoles on (left), CW sextupoles off (right).

DAΦNE UPGRADE

During a six months shut-down in 2007, DAΦNE has been modified to implement the large piwinsky angle configuration. The collider has been turned on again in Dec-2007 and the machine has been running until May-2008. A new experiment called Siddharta has been installed at the IP and has been taking data since March-2008. The new beam parameters are summarized in Table 1. For comparison, the parameters used during the last DAΦNE run with the KLOE detector (2005-2006) are also shown.

Table 1. Comparison of beam parameters for KLOE run (2006) and for DAΦNE upgrade for SIDDHARTA run

Parameters	KLOE	Siddharta Design	Siddharta Achieved
L ($\text{cm}^{-2} \text{s}^{-1}$)	1.5×10^{32}	$>5.0 \times 10^{32}$	$>2.2 \times 10^{32}$
N_{bunch}	110	110	95
$N_{\text{part/bunch}}$	2.65×10^{10}	2.65×10^{10}	2.65×10^{10}
I_{bunch} (mA)	13.	13.	11.
ϵ_x (nm)	300.	200.	260.
ϵ_y (nm)	1.5	1.	1.25
Coupling (%)	0.5	0.5	0.5
σ_x (μm)	700.	200.	260.
σ_y (μm)	15 (blow up)	2.4	4.0
σ_z (mm)	25.	20	20
β_x (m)	1.5	0.2	0.26
β_y (mm)	18.	6.	10.5
θ (mrad)	2×16	2×25	2×25

LUMINOSITY RESULTS

The most relevant results of the commissioning concern the luminosity. So far the maximum measured peak luminosity is in excess of $L_{\text{peak}} = 2.2 \cdot 10^{32} \text{ cm}^{-2} \text{ s}^{-1}$, the best daily integrated luminosity is $L_{\text{fday}} \sim 8 \text{ pb}^{-1}$ and the highest integrated luminosity in one hour is $L_{\text{f1hour}} \sim 0.5 \text{ pb}^{-1}$ averaged over a two hours run (see Fig. 3).

01 Circular Colliders

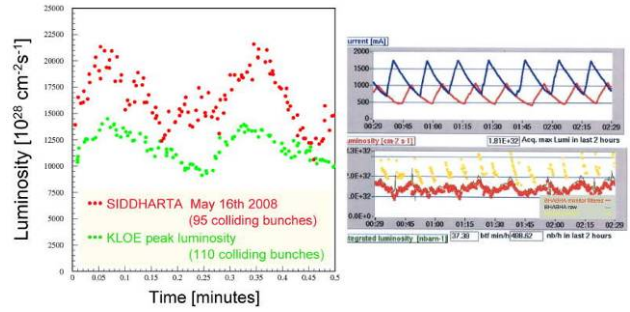


Figure 3: Peak luminosity (left) and integrated luminosity (right) over 2 hours.

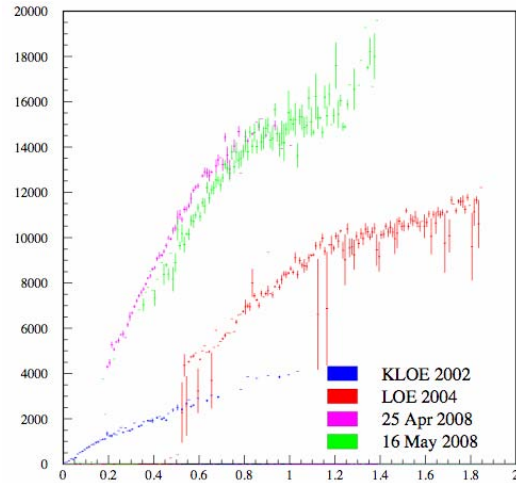


Figure 4: Peak luminosity ($\cdot 10^{28} \text{ cm}^{-2} \text{ s}^{-1}$) vs currents product (Amps^2) for the KLOE run and for the Siddharta run.

These results have been obtained without reaching the low beta parameters and the CW sextupole strength to their nominal values (now running at about 50% of the theoretical geometric value). The present vertical size increase w.r.t. the low current one is about 60%; 30% is due to single beam effects, ion trapping electron cloud and HOM instabilities, 30% is due to beam-beam. In order to reduce the beam-beam blowup, we plan further squeeze in β_y^* and a 30% increase in the CW sextupoles strength in the near future. Moreover the number of colliding bunches will gradually increase from 95 to 110 as the vacuum conditioning proceeds, this should also mitigate the ion-trapping and electron cloud blowup. The peak luminosity is foreseen to reach $4.0 \cdot 10^{32} \text{ cm}^{-2} \text{ s}^{-1}$ and the monthly integrated luminosity $\sim 0.5 \text{ fb}^{-1}$ by the end of the Siddharta run.

SUPER-B DESIGN

The construction and operation of modern multi-bunch e^+e^- colliders [1,2,3] have brought about many advances in accelerator physics in the area of high currents, complex interaction regions, high beam-beam tune shifts,

A14 Advanced Concepts

high power RF systems, controlled beam instabilities, rapid injection rates, and reliable uptimes (~90%):

A Conceptual Design Report (CDR) [5] was issued in May 2007, with about 200 pages dedicated to the accelerator design. This report discusses site requirements, crab waist compensation, parameters optimization in order to save power, IP quadrupole design, Touschek backgrounds, spin rotator scheme, and project costs. A possible layout at Tor Vergata University near Rome is shown in Fig. 5. The ring lattices have been modified to produce very small horizontal (a few nm-rad) and vertical emittances (a few pm-rad).

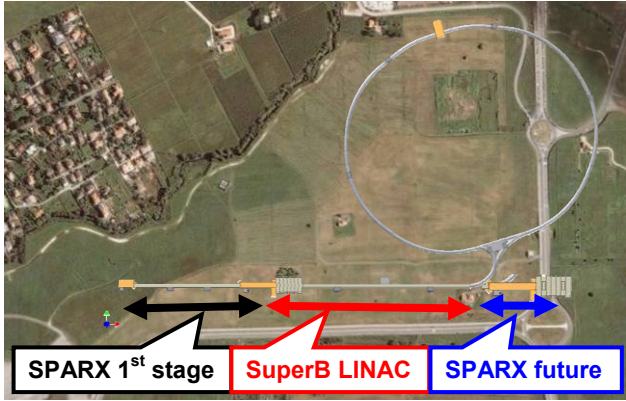


Figure 5: Possible SuperB location at Tor Vergata University with a ring circumference of 1800 m and an injector located adjacent to the future SPARX FEL.

SUPER-B PARAMETERS

The Super-B accelerator consists of two asymmetric energy rings, colliding in one Interaction Region (IR) at a large horizontal angle, with a spin rotator section in the HER to provide longitudinal polarization of the electron beam at the IP. In order to have equal tune shifts for the two beams, asymmetric B-Factories operate at unbalanced beam currents, with a current ratio inverse to the energy ratio. For SuperB, with an energy ratio of 7/4 and a large crossing angle, new conditions for having equal tune shifts are possible. LER (+) and HER (-) beams can have different emittances and β^* but equal currents:

$$\xi^+ = \xi^- \Leftrightarrow \frac{\beta_y^+}{\beta_y^-} = \frac{E^+}{E^-} \quad (1)$$

Then, in order to have equal vertical beam sizes at IP, the LER and HER vertical and horizontal emittances must be:

$$\varepsilon_y^+ = \frac{E^-}{E^+} \varepsilon_y^-, \quad \varepsilon_x^+ = \frac{E^-}{E^+} \varepsilon_x^- \quad (2)$$

with the horizontal beam sizes in the inverse ratio with the beam energies. Thus, the LER beam sees a shorter interaction region, in a ratio 4/7, with respect to the HER beam. This allows for further β_y^* reduction, a larger

emittance, increased the Touschek lifetime, and reduced the injection rates. Table 2 summarizes Super-B beam parameters for the three operational scenarios. Fig. 2 shows the left-right crab waist compensation at the IP. Fig. 6 shows the beam cross sections at the IP with unequal emittances but equal beam-beam tune shifts.

Table 2: SuperB main parameters

Parameter (LER/HER)	Nominal	Upgrade	Ultimate
Energy (GeV)	4/7	4/7	4/7
Luminosity ($\text{cm}^{-2}\text{s}^{-1}$)	1×10^{36}	2×10^{36}	4×10^{36}
C (m)	1800	1800	1800
N. of bunches	1251	1251	2502
F_{RF} (MHz)	476	476	476
N. part/bunch	5.5×10^{10}	5.5×10^{10}	6.8×10^{10}
I_{beam} (A)	1.85/1.85	1.85/1.85	3.7/3.7
β_x^* (mm)	35/20	35/20	35/20
β_y^* (mm)	0.22/0.39	0.16/0.27	0.16/0.27
ε_x^* (nm rad)	2.8/1.6	1.4/0.8	1.4/0.8
ε_y^* (pm rad)	7/4	3.5/2	3.5/2
σ_x^* (μm)	10/5.7	7/4	7/4
σ_y^* (μm)	0.039	0.023	0.023
σ_z (mm)	6.	6.	6.
θ_{cross} (mr)	48	48	48
α_c ($\times 10^{-4}$)	3.2/3.8	3.2/3.8	3.2/3.8
$\tau_{x,y}/\tau_s$ (ms)	40/20	28/14	28/14
x-tune shift	0.004/0.003	0.006/0.003	0.006/0.003
y-tune shift	0.15	0.20	0.20
RF power (MW)	26	54	64

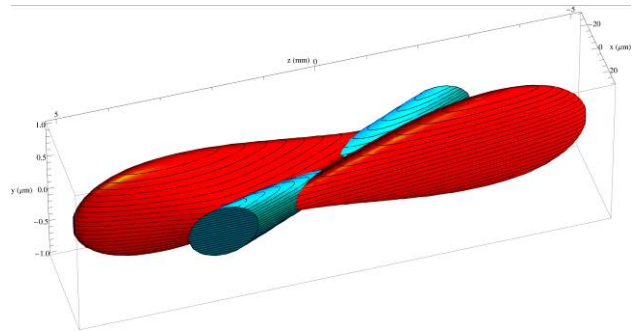


Figure 6: Beam cross sections at the IP with parameters from Table 1 and crab waists.

SUPER-B FACTORY LAYOUT

The two rings each have four arcs, one long straight section for diagnostics, RF and injection, two short straight sections for damping wigglers (optional) and a Final Focus section that also provides about 35degrees of total bend angle. The Crab Sextupoles are located just at the end of the Final Focus section. Good dynamic apertures have been found with the crab waist sextupoles [6] as shown in Fig. 7.

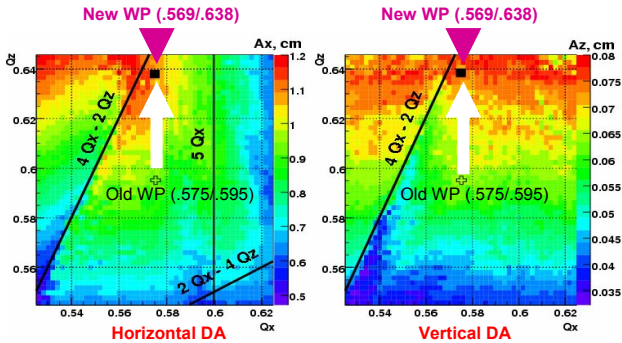


Figure 7: Dynamic aperture with crab waist versus horizontal and vertical tune used to find the optimum tune plane locations. Red is better and blue is worse.

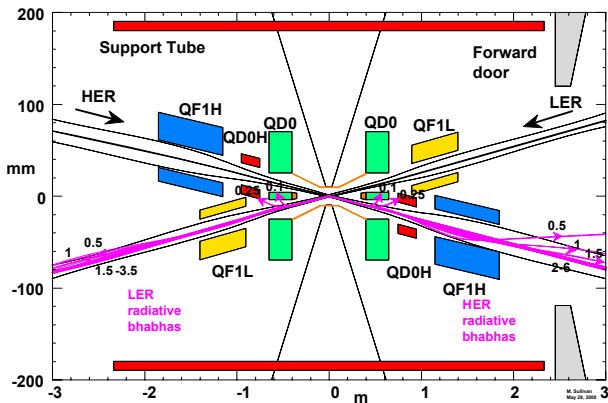


Figure 8: Interaction region for two asymmetric beams.

INTERACTION REGION PARAMETERS

The interaction region (Fig. 8) is designed to be similar to that of the ILC and to leave about the same longitudinal free space for the detector as that presently used by BABAR or BELLE, but with superconducting quadrupole doublets QD0/QF1 as close to the interaction region as possible [13,14]. The total FF length is about 160 m and the final doublet is at 0.5m from the IP. A plot of the optical functions in the incoming half of the FF region is presented in Fig. 9. The choice for a finite crossing angle at the IP greatly simplifies the IR design, naturally separating the beams at the parasitic collisions. The resulting vertical beta is about 0.2-0.3 mm and the horizontal 35 mm. These beta values are much closer to a linear collider design than a traditional circular collider. The beams enter the interaction point nearly straight to minimize synchrotron radiation and lost particle

backgrounds. The beams are bent more while exiting the IR to avoid parasitic collisions and the resulting beam-beam effects.

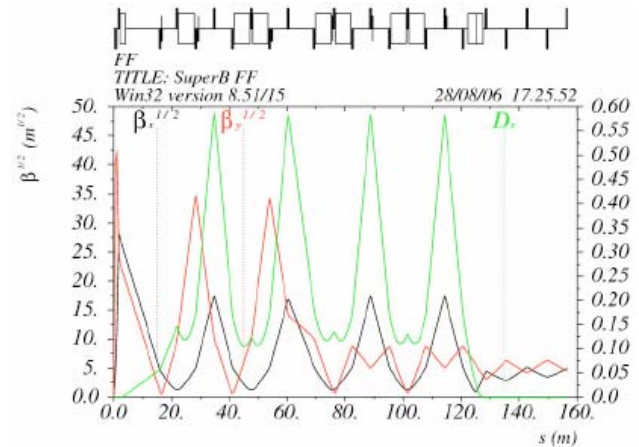


Figure 9: IR optical parameters for a Super-B-Factory.

POWER REQUIREMENTS

The power required for this collider is the sum of power for the magnets, RF system, cooling water, controls, and the accelerator operation. The present estimates indicate about 25 MW is needed for the nominal case. These values do not include the campus power requirements or that of the particle physics detector. There are upgrade possibilities for this collider to 2 to 4 times the design luminosity that will require more power [15]. Due to the advantages of the very low emittances and the crab waist with this design, the power requirements are significantly lower than those of the present B-Factory colliders.

INJECTION REQUIREMENTS

The injection system needed for the Super-B is similar to that for PEP-II, shown in Fig. 10. Table 3 shows the basic injector parameters. Since the beam lifetimes are of the order of 10 minutes, continuous injection is needed. The injector will operate at 100 Hz and inject about 2 bunches per pulse. The values shown here are for the upgraded collider at higher luminosity.

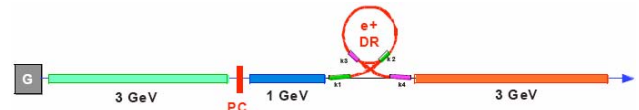


Figure 10: Schematic of the Super-B injector.

Table 3 Super-B Injection Parameters

Parameter	Unit	e+	e-
Linac energy	GeV	4	7
Damping ring energy	GeV	1	1
Linac frequency	MHz	2856	2856
Bunches per pulse		2	2
Injection efficiency	%	67	85
Pulse rate per beam	Hz	75	25
Injected particles/pulse	10 ¹⁰	4	5.1
Injection rate total	10 ¹² /sec	2.0	2.6

SUPERB BEAM-BEAM SIMULATIONS

Beam-beam studies for SuperB started with a beam parameters set similar to that of the ILC damping ring. Numerical simulations with LIFETRAC have shown that the design luminosity of $10^{36} \text{ cm}^{-2}\text{s}^{-1}$ is achieved already with $2\text{-}2.5 \times 10^{10}$ particles per bunch. According to the simulations, for this bunch population the beam-beam tune shift is well below the maximum achievable value. Indeed, as one can see in Fig. 11, the luminosity grows quadratically with the bunch intensity till about 7.5×10^{10} particles per bunch. We have used this safety margin to significantly relax and optimize many critical parameters, including damping time, crossing angle, number of bunches, bunch length, bunch currents, emittances, beta functions and coupling, while maintaining the design luminosity of $10^{36} \text{ cm}^{-2}\text{s}^{-1}$.

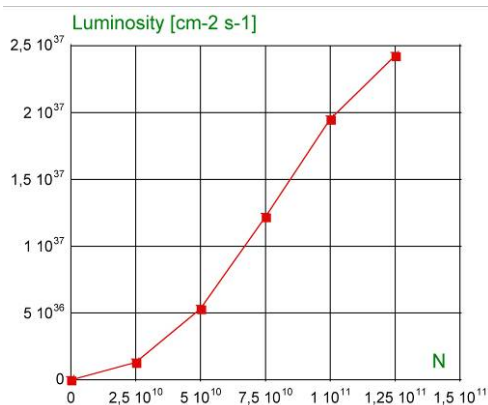


Figure 11: SuperB luminosity versus bunch intensity.

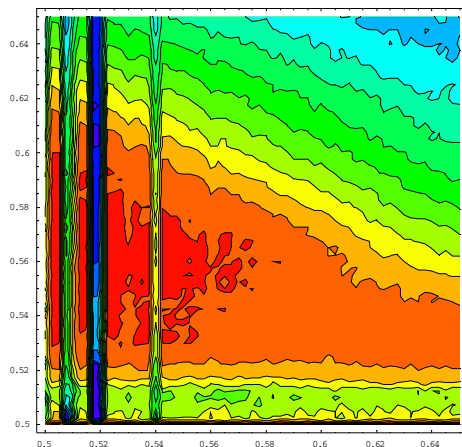


Figure 12: SuperB luminosity tune scan (horizontal axis - v_x from 0.5 to 0.65; vertical axis - v_y from 0.5 to 0.65).

In order to define how large is the “safe” area with the design luminosity, a luminosity tune scan has been performed for tunes above the half integers, which is typical for the operating B-factories. The resulting 2D contour plot is shown in Fig. 12. Individual contours differ by 10% in luminosity. The maximum luminosity found inside the scanned area is $1.21 \times 10^{36} \text{ cm}^{-2}\text{s}^{-1}$, while the minimum one is as low as $2.25 \times 10^{34} \text{ cm}^{-2}\text{s}^{-1}$. We can conclude that the design luminosity can be obtained over a wide tune area. It has also been found numerically that for the best working points the distribution tails growth is negligible.

CONCLUSIONS

The DAΦNE collider has been successfully commissioned in the new “Crab-Waist” mode and is presently delivering luminosity to the SIDDHARTA prototype detector. The final detector will be installed next August. Peak and average luminosity are already sufficient to perform the experiment in few months.

Further improvements of machine operation are likely to fulfill the requirements for a future roll-in of the KLOE detector.

The numerical simulations indicate that by exploiting the crab waist scheme the luminosity of the low emittance Super B-factory can be as high as $10^{36} \text{ cm}^{-2}\text{s}^{-1}$.

REFERENCES

- [1] P. Raimondi, 2nd SuperB Workshop, Frascati, 2006.
- [2] D. Alesini et al., LNF-06/33 (IR), 2006.
- [3] C. Milardi et al., TUPAN033, this conference.
- [4] M. Biagini et al., MOOBKI02, this conference.
- [5] SuperB CDR, INFN/AE-07/2, SLAC-R-856, 2007.
- [6] D. Shatilov and M. Zobov, ICFA BDN 37, 99 (2005).
- [7] D. Pestrikov, Nucl.Instrum.Meth. A336, 427 (1993).
- [8] J. Seeman, PAC05, p. 2333.
- [9] H. Koiso, PAC05, p. 64.
- [10] DANAE Letter of Intent, see <http://www.lnf.infn.it>.
- [11] K. Ohmi et al., PRSTAB 7, 104401 (2004).
- [12] P. Raimondi et al., e-Print:physics/0702033, 2007.
- [13] M. Sullivan et al, “Super-B interaction region design,” EPAC 2008.
- [14] E. Paoloni et al, “IR SC quadrupole design for Super-B,” EPAC 2008.
- [15] U. Wienands, S. Nikitin et al, Super-B Elba meeting, <https://agenda.infn.it/conferenceDisplay.py?confId=347>.